nature medicine

ARTICLES

ERK activation drives intestinal tumorigenesis in *Apc*$^{min/+}$ mice

Sung Hee Lee[1,3], Li-Li Hu[1], Jose Gonzalez-Navajas[1], Geom Seog Seo[1,3], Carol Shen[1], Jonathan Brick[1], Scott Herdman[1], Nissi Varki[2], Maripat Corr[1], Jongdae Lee[1] & Eyal Raz[1]

Toll-like receptor (TLR) signaling is essential for intestinal tumorigenesis in *Apc*$^{min/+}$ mice, but the mechanisms by which Apc enhances tumor growth are unknown. Here we show that microflora-MyD88-ERK signaling in intestinal epithelial cells (IECs) promotes tumorigenesis by increasing the stability of the c-Myc oncoprotein. Activation of ERK (extracellular signal–related kinase) phosphorylates c-Myc, preventing its ubiquitination and subsequent proteasomal degradation. Accordingly, *Apc*$^{min/+}$/*Myd88*$^{-/-}$ mice have lower phospho-ERK (p-ERK) levels and fewer and smaller IEC tumors than *Apc*$^{min/+}$ mice. MyD88 (myeloid differentiation primary response gene 88)-independent activation of ERK by epidermal growth factor (EGF) increased p-ERK and c-Myc and restored the multiple intestinal neoplasia (Min) phenotype in *Apc*$^{min/+}$/*Myd88*$^{-/-}$ mice. Administration of an ERK inhibitor suppressed intestinal tumorigenesis in EGF-treated *Apc*$^{min/+}$/*Myd88*$^{-/-}$ and *Apc*$^{min/+}$ mice and increased their survival. Our data reveal a new facet of oncogene-environment interaction, in which microflora-induced TLR activation regulates oncogene expression and related IEC tumor growth in a susceptible host.

The gastrointestinal tract is constantly exposed to vast numbers of commensal bacteria and their inflammatory products. Essential to intestinal homeostasis are pattern recognition receptors (PRRs) such as TLRs[1]. Engagement of TLRs with their cognate ligands in the intestinal mucosa provokes the production of proinflammatory, proangiogenic and other growth factors that support IEC differentiation and proliferation[2]. In a genetically susceptible host, ongoing intestinal inflammation triggers uncontrolled growth of IECs, leading to neoplasia[3–5]. Likewise, it has been proposed that signaling through the TLR-MyD88 pathway regulates IEC tumor development in mice heterozygous for a mutant form of the tumor suppressor gene *Apc* (encoding adenomatous polyposis coli)[6]. However, the underlying pro-tumorigenic mechanisms of TLR signaling have not been identified. The *Apc*$^{min/+}$ mouse is an animal model of human familial adenomatous polyposis[7]. These mice develop multiple intestinal neoplasia (Min) after they spontaneously lose the heterozygous wild-type *Apc* allele in certain IECs, and consequently die by the time they reach 6 months of age[8].

The survival and growth of some tumors are dependent on the continued activation of oncogenes. This phenomenon, known as 'oncogene addiction,' explains tumor suppression that occurs as a result of the inactivation of a single gene product[9]. The oncogene *c-Myc* is crucial for *Apc*-mediated tumorigenesis[10,11]. The genetic deletion of *c-Myc* in IEC of *Apc*$^{min/+}$ mice results in the inhibition of tumor growth[11], and reduction of c-Myc expression in IECs by as little as a factor of 2 is sufficient to inhibit tumorigenesis in these mice[12–14]. We determined that MyD88-dependent activation of ERK in IECs is essential for intestinal tumor growth in *Apc*$^{min/+}$ mice via the stabilization of c-Myc protein. Consequently, the inhibition of p-ERK abrogates the Min phenotype in these mice.

RESULTS

MyD88 signaling is essential for polyp growth in *Apc*$^{min/+}$ mice

TLRs signal mainly through either MyD88 or Toll-like receptor adaptor molecule 1 (TRIF, also known as TICAM). To explore the potential impact of TLR signaling on IEC tumors, we therefore crossed *Apc*$^{min/+}$ mice to *Myd88*$^{-/-}$ or to *Ticam*$^{Lps2/Lps2}$ (*Lps2*) mice[15]. The average survival was 23 weeks for *Apc*$^{min/+}$ mice and 28 weeks for *Apc*$^{min/+}$/*Lps2* mice. In contrast, all of the *Apc*$^{min/+}$/*Myd88*$^{-/-}$ mice survived the 45-week study (**Supplementary Fig. 1a**). We then determined the role of each adaptor protein in tumor (polyp) formation at in mice at 20 weeks of age. *Apc*$^{min/+}$/*Myd88*$^{-/-}$ mice had fewer polyps throughout the small and large intestines than *Apc*$^{min/+}$ or *Apc*$^{min/+}$/*Lps2* mice (**Supplementary Fig. 1b**,**c**), but they showed circular raised lesions (microadenomas) in both the distal small intestine (DSI) and the colon (**Supplementary Fig. 1c**–**f**).

MyD88 signaling regulates proliferation and apoptosis of IECs

As the polyps in the *Apc*$^{min/+}$/*Myd88*$^{-/-}$ mice failed to grow (**Supplementary Fig. 1c**), we investigated whether the deletion of *Myd88* affected IEC proliferation. The proliferation and migration rates of IEC along the crypt-villus axis, as measured by BrdU incorporation, were lower than in *Apc*$^{min/+}$ mice (**Fig. 1a**). We also observed a significantly higher number of apoptotic IECs in *Apc*$^{min/+}$/*Myd88*$^{-/-}$

[1]Department of Medicine, University of California, San Diego, La Jolla, California, USA. [2]Department of Pathology, University of California, San Diego, La Jolla, California, USA. [3]Current addresses: College of Pharmacy, Wonkwang University, Iksan, Chonbuk, Republic of Korea (S.H.L.); Wonkwang University School of Medicine, Iksan, Chonbuk, Republic of Korea (G.S.S.). Correspondence should be addressed to E.R. (eraz@ucsd.edu).

Received 18 October 2009; accepted 1 April 2010; published online 9 May 2010; doi:10.1038/nm.2143

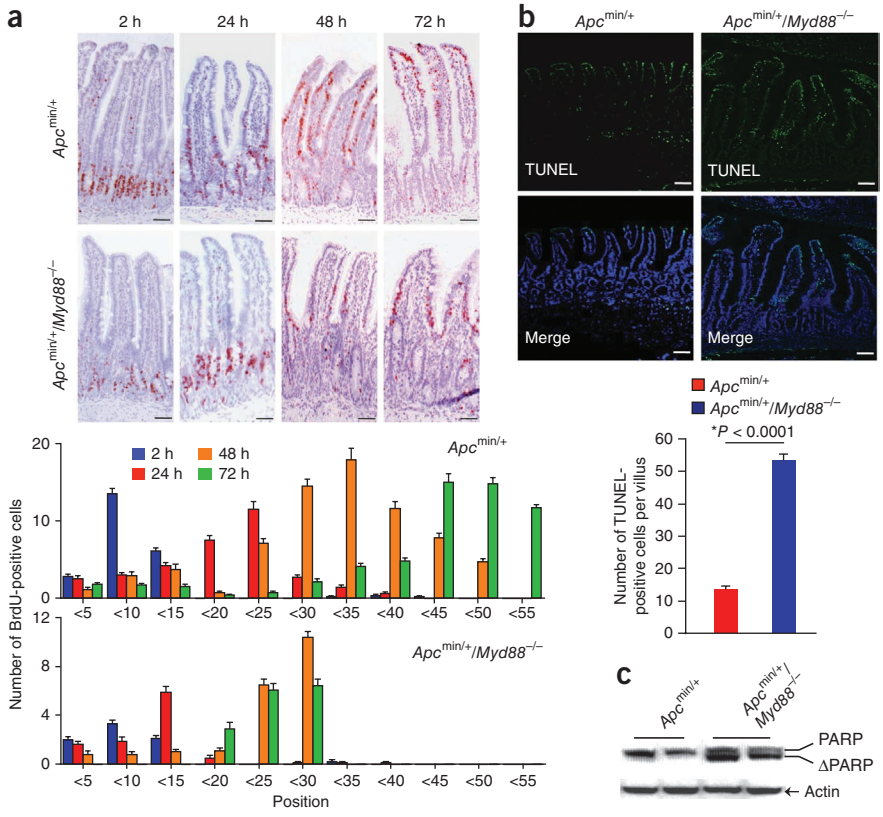

Figure 1 Genetic disruption of *Myd88* in $Apc^{min/+}$ mice suppresses proliferation and enhances apoptosis of IECs. (**a**) IHC and BrdU incorporation in IECs (DSI) after intraperitoneal (i.p.) BrdU injection (scale bars, 20 μm; magnification, ×200). BrdU-positive cells, per time point, were enumerated for each indicated position in a crypt (10 crypt-villi units per time point), with position 0 being the base of the crypt[39]. (**b**) Apoptotic IECs (DSI) were determined by TUNEL assay (scale bars, 40 μm; magnification, ×100). (**c**) Cleaved product of poly(ADP-ribose) polymerase (PARP) in IECs (DSI) harvested from the indicated mice ($n = 2$ per group). Error bars represent s.d.

(**Fig. 1b**) as well as an increase in cleaved poly(ADP-ribose) polymerase (PARP), a substrate of caspase-3 (ref. 16) (**Fig. 1c**). Together, these data indicate that TLR signaling by MyD88 enhances IEC proliferation and inhibits IEC apoptosis, and suggest that these two effects synergize in enhancing IEC tumor growth in $Apc^{min/+}$ mice.

MyD88 signaling in IEC controls IEC tumor growth

In the intestinal mucosa, both IEC and bone marrow–derived cells have functional TLRs that use MyD88 for signaling[17–19]. To further clarify the role of bone marrow–derived cells in IEC tumorigenesis, we generated bone marrow chimeras by reconstituting both $Apc^{min/+}$ and $Apc^{min/+}/Myd88^{-/-}$ recipients with bone marrow harvested from either WT or $Myd88^{-/-}$ donors[20]. Reconstitution of $Apc^{min/+}$ recipients with either $Myd88^{-/-}$ or WT bone marrow did not significantly alter polyp count and growth in either the DSI or the colon. Similarly, the number of polyps did not change significantly in $Apc^{min/+}/Myd88^{-/-}$ recipients reconstituted with WT or $Myd88^{-/-}$ bone marrow (**Fig. 2a**). These results indicate that polyp growth in $Apc^{min/+}$ mice does not depend on TLR-MyD88 signaling in bone marrow–derived cells, and strongly suggest that it instead depends on TLR-MyD88 activation of IECs.

To explore whether host-derived or microbial-derived TLR ligands play a role in IEC tumorigenesis, we crossed $Apc^{min/+}$ mice with $Il1r1^{-/-}$ or with $Casp1^{-/-}$ mice, which are limited in processing interleukin (IL)-1 and IL-18 (ref. 21). There was no significant difference in the numbers of polyps in $Apc^{min/+}/Il1r1^{-/-}$ or $Apc^{min/+}/Casp1^{-/-}$ as compared to $Apc^{min/+}$ mice (**Fig. 2b**). In addition, administration of the IL-1R antagonist anakinra did not affect the extent of IEC tumorigenesis in $Apc^{min/+}$ mice (**Fig. 2c**). Collectively, these data strongly suggest that MyD88-dependent TLR activation by microbial ligands is responsible for IEC tumor growth in $Apc^{min/+}$ mice.

A MyD88-dependent TLR signaling upregulates c-Myc in IECs

The decrease in IEC proliferation and the increase in IEC apoptosis in $Apc^{min/+}/Myd88^{-/-}$ mice suggested that a MyD88-dependent oncogene or mitogen is involved in IEC tumorigenesis. Because c-Myc is essential for tumorigenesis in $Apc^{min/+}$ mice[11,12,14], we tested whether MyD88 regulates c-Myc expression. MyD88 deficiency resulted in a significant decrease in c-Myc protein in IECs. Whereas c-Myc was expressed throughout the crypt in both the DSI and the colon of $Apc^{min/+}$ mice, its expression in $Apc^{min/+}/Myd88^{-/-}$ mice was restricted to the base of the crypt (**Fig. 3a**). Immunoblotting analysis of c-Myc in isolated IECs (in the DSI) confirmed the reduced expression of not only c-Myc, but also p-ERK, in $Apc^{min/+}/Myd88^{-/-}$ mice (**Fig. 3b** and **Supplementary Fig. 2a**). Decreased c-Myc expression in $Apc^{min/+}/Myd88^{-/-}$ IEC was observed in both normal and tumor regions (**Supplementary Fig. 2b**). Nevertheless, the c-Myc mRNA levels in IECs did not differ significantly between $Apc^{min/+}$ and $Apc^{min/+}/Myd88^{-/-}$ mice (**Fig. 3c**). Inactivation of *Apc* activates β-catenin, which induces transcription of c-Myc. The deletion of *Myd88* did not affect β-catenin abundance *in vivo* (**Fig. 3b**) or Wnt3 (wingless-related MMTV integration

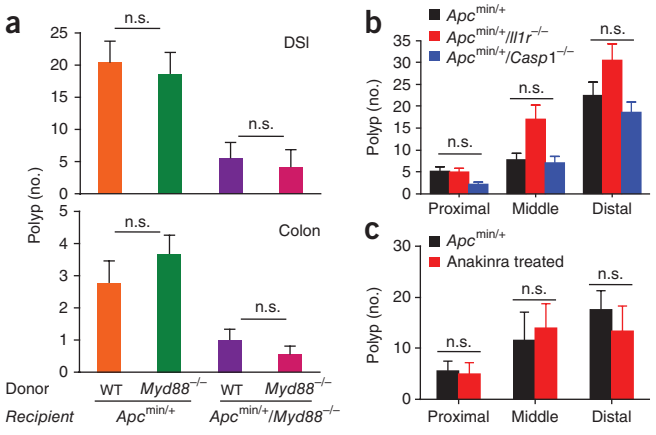

Figure 2 Myd88 signaling in hematopoietic cells is not required for tumorigenesis in $Apc^{min/+}$ mice. (**a**) Polyp count in bone marrow chimeras in the DSI and colon ($n = 7$–9 mice per group); n.s., nonsignificant. (**b**) Polyp count in the small intestine in $Apc^{min/+}/Il1r1^{-/-}$ and $Apc^{min/+}/Casp1^{-/-}$ mice at 20 weeks of age ($n = 7$ per group). (**c**) Polyp count in anakinra-treated $Apc^{min/+}$ mice (DSI) ($n = 7$ per group). $P < 0.05$.

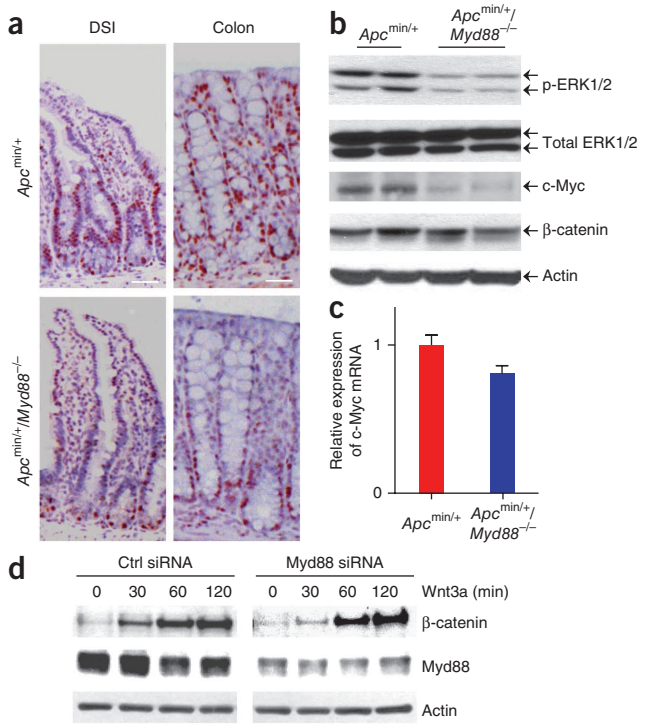

Figure 3 MyD88 regulates c-Myc expression levels. (**a**) IHC analysis of c-Myc protein in IECs from the DSI and colon from 20-week-old mice (scale bars, 10 μm; magnification, ×200). (**b**) Immunoblot analysis of the indicated proteins in IECs (DSI) of 20-week-old mice ($n = 2$). (**c**) Transcript abundance of *Myc* in IECs (DSI) (nonsignificant; $n = 3$ per group). Error bars represent s.d. (**d**) RKO cells transfected with either control or *Myd88* siRNA, stimulated with Wnt3a (100 ng ml^{-1}) and subjected to immunoblot analysis.

site 3)-induced activation of β-catenin *in vitro* (**Fig. 3d**). These data indicate that MyD88 signaling affects tumorigenesis independently of the Wnt–APC–β-catenin pathway.

Post-translational modification of c-Myc by ERK

Our data suggest that MyD88-mediated signaling in IEC causes tumor growth. Because IECs express functional TLRs[18,19] (**Supplementary Fig. 3a**), we tested whether activation of a TLR-MyD88 pathway directly induces c-Myc expression. Indeed, TLR2 activation did enhance the abundance of c-Myc protein in the IEC line RKO (*Apc* wild type) (**Fig. 4a**) in a MyD88-dependent manner (**Supplementary Fig. 3b**). Activation of TLR5 (a MyD88-dependent TLR) in RKO produced a similar result (**Supplementary Fig. 3c**). Consistent with mRNA levels observed *in vivo* (**Fig. 3c**), the level of c-Myc mRNA was not affected by TLR2 triggering, whereas expression of IL-8 and IκBα were increased[19] (**Fig. 4a**).

The increase in c-Myc protein without a concomitant increase in mRNA level after TLR stimulation suggested that c-Myc protein is subjected to post-translational modifications[22]. Indeed, inhibition of proteasomal function by MG-132 increased c-Myc protein in RKO cells without affecting the mRNA level (**Fig. 4b**), indicating a steady-state degradation of c-Myc. We therefore tested whether TLR stimulation in IECs stabilizes c-Myc protein. Although the c-Myc–ubiquitin conjugates were easily detected even in the absence of a proteasome inhibitor in RKO cells, they disappeared rapidly upon TLR2 stimulation with a concomitant increase in unconjugated c-Myc protein (**Fig. 4c**). Accordingly, these results suggest that the TLR-MyD88–mediated signaling pathway stabilizes c-Myc protein in IEC by inhibiting its proteasomal degradation.

The MEK-ERK pathway phosphorylates c-Myc on Ser62, which stabilizes c-Myc by preventing ubiquitination and proteasomal degradation[23–25]. We examined whether Myd88-mediated activation of ERK is responsible for the stabilization of c-Myc. TLR2 activation did induce the phosphorylation of ERK as well as that of c-Myc on Ser62 (**Fig. 4a**). In addition, blocking ERK activation with pharmacological inhibitors rapidly reduced c-Myc abundance (**Fig. 4d**). Caco-2, another IEC line, expresses a truncated APC protein similar to that observed in *Apc*$^{min/+}$ mice[26]. We therefore tested whether MyD88-dependent ERK activation can stabilize c-Myc in these *Apc* mutant cells. TLR2 stimulation increased c-Myc protein abundance with a concomitant ERK activation and decrease in the polyubiquitinated c-Myc (**Supplementary Fig. 4a**,**b**). Similarly, stimulation of either TLR2 or the epidermal growth factor receptor (EGFR) in a non-transformed IEC line derived from the small intestine (RIE-1) also activated ERK and c-Myc (**Supplementary Fig. 4c**). Thus, c-Myc in *Apc*$^{min/+}$ mice is maintained by two independent mechanisms: a transcriptional activation of c-Myc by β-catenin signaling initiated by Apc inactivation and a post-translational stabilization of c-Myc by MyD88-dependent ERK activation.

ERK signaling drives the Min phenotype

We tested whether a MyD88-independent activation of ERK increases c-Myc protein amounts in *Apc*$^{min/+}$/*Myd88*$^{-/-}$ mice and restores the Min phenotype. As EGF activates ERK and enhances c-Myc abundance

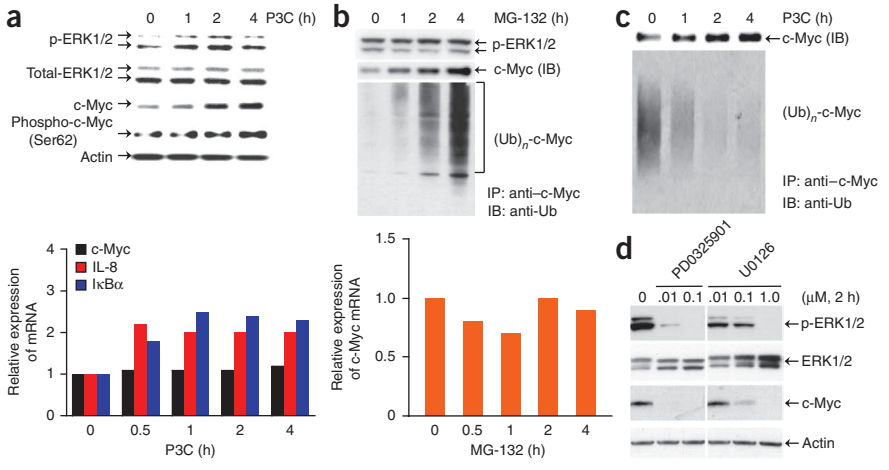

Figure 4 TLR signaling via MyD88 stabilizes c-Myc protein in IECs through activation of ERK. (**a**) RKO cells stimulated with P3C (2 μg ml^{-1}), lysed and analyzed by immunoblotting (IB; top) and transcript levels (qPCR) after TLR2 stimulation (bottom). (**b**) Abundance of protein (IB; top) and transcript (qPCR; bottom) in MG-132 treated (10 μM) RKO cells. c-Myc was immunoprecipitated (IP) and then subjected to IB with anti-ubiquitin (Ub) antibody. (**c**) RKO cells were treated with P3C (2 μg ml^{-1}), and the abundance of ubiquitinated c-Myc was measured by IP followed by IB. (**d**) p-ERK and c-Myc abundance (IB) in U0126- or PD0325901-treated RKO cells.

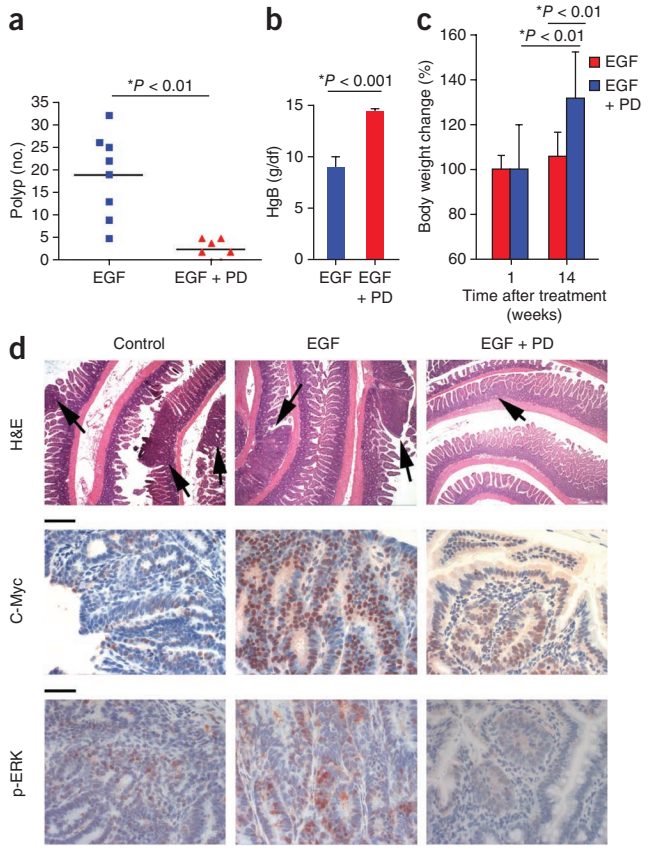

Figure 5 Activation of ERK restores the Min phenotype in *Apc*$^{min/+}$/*Myd88*$^{-/-}$ mice. (**a**) PD reduces the number of polyps in EGF-treated *Apc*$^{min/+}$/*Myd88*$^{-/-}$ mice (DSI) ($n = 8$ per group). (**b**,**c**) Blood hemoglobin concentrations (**b**) and body weight (**c**) of these mice. (**d**) Top, H&E of DSI in control, EGF-treated and EGF + PD–treated mice. The arrows indicate intestinal polyps. Middle, c-Myc expression in IEC. Bottom, p-ERK levels in IECs. Error bars represent s.d.

in non-transformed IECs (**Supplementary Fig. 4c**), we treated *Apc*$^{min/+}$/*Myd88*$^{-/-}$ mice either with EGF alone or with EGF plus a MEK1/2 inhibitor (PD0325901, PD). The latter is a specific and effective pharmacological inhibitor of ERK[27] and is in phase 2 clinical trials in cancer. The administration of EGF significantly increased the number of polyps in the DSI (see **Supplementary Fig. 1b**), but this induction was abrogated by PD treatment (**Fig. 5a**). Serum hemoglobin and body weights drop significantly in *Apc*$^{min/+}$ mice over time as a result of increasingly large and abundant exophytic polypoid intestinal tumors that minimize food absorption and cause subsequent intestinal obstruction and bleeding[28]. The inhibition of tumor growth in PD-treated *Apc*$^{min/+}$/*Myd88*$^{-/-}$mice coincided with increased serum hemoglobin concentrations (**Fig. 5b**) and increased body weight (**Fig. 5c**), indicative of better health. As expected, EGF administration enhanced the abundance of c-Myc and p-ERK in IECs, which was reversed by PD treatment (**Fig. 5d**). Hence, the inhibition of IEC tumors in PD-treated mice further validated the regulatory role of ERK on tumorigenesis in *Apc*$^{min/+}$/*Myd88*$^{-/-}$ mice (**Fig. 3b**) and may suggest that the TLR-MyD88 pathway is a major contributor to ERK activation in *Apc*$^{min/+}$ mice in steady-state conditions. These results suggest a pivotal role for ERK activation of the Min phenotype. We therefore tested its tumorigenic role in 10-week-old *Apc*$^{min/+}$ mice. PD treatment of these mice for 14 weeks resulted in complete inhibition of polyp growth (**Fig. 6a**) with an associated increase in serum hemoglobin concentrations (**Fig. 6b**) and body weight (**Fig. 6c**). PD treatment also inhibited both c-Myc and p-ERK in IECs of these mice (**Fig. 6d**,**e**). Furthermore, in another study, PD treatment of 10-week-old *Apc*$^{min/+}$ mice resulted in 100% survival, whereas treatment with vehicle resulted in 100% mortality during the following 17-week treatment period (**Fig. 6f**). To detect the long-term effects of PD treatment, we continued to deliver it or vehicle to

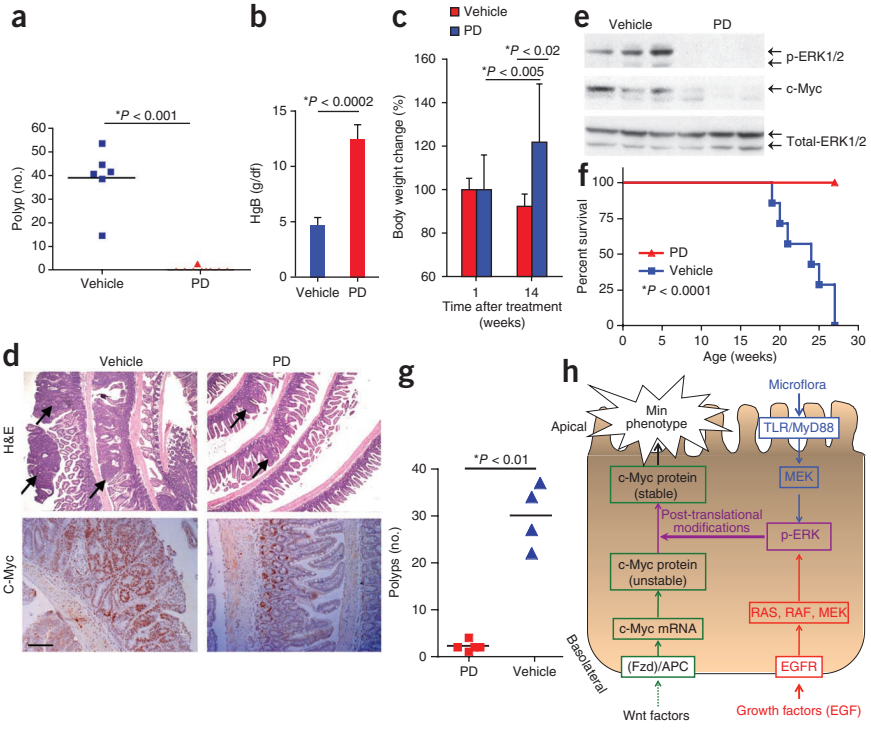

Figure 6 Activation of ERK is essential for the Min phenotype in *Apc*$^{min/+}$ mice. (**a**–**c**) Polyp count (**a**), hemoglobin level (**b**) and body weight (**c**) in PD-treated *Apc*$^{min/+}$ mice ($n = 6$ for vehicle, $n = 9$ for PD group). (**d**) Top, H&E of DSI in control and PD-treated *Apc*$^{min/+}$ mice. Arrows indicate intestinal polyps. Bottom, c-Myc expression in IECs. (**e**) Immunoblot analysis of c-Myc and p-ERK levels in IECs (DSI) of these mice. (**f**) Survival in PD-treated or vehicle-treated *Apc*$^{min/+}$ mice for 17 weeks ($n = 8$). (**g**) The PD-treated *Apc*$^{min/+}$ mice in **f** were split to PD- and vehicle-treated groups ($n = 4$ per group). Polyp count (DSI) was performed 15 weeks later. (**h**) Microflora induces tumorigenesis in *Apc*$^{min/+}$ mice by triggering the TLR-ERK pathway in IECs. This stabilizes c-Myc and inhibits its proteasomal degradation. Increased c-Myc levels induce the Min phenotype. Additional signals such as growth factors use the MEK-ERK pathway and, like TLR ligands, can enhance c-Myc expression. However, sterile food and water contain TLR ligands (for example, lipopolysaccharides) that are capable of stimulating IECs. This may account for the Min phenotype observed in *Apc*$^{min/+}$ mice housed under germ-free conditions[40]. Error bars represent s.d.

PD-treated *Apc*$^{min/+}$ mice for an additional 15 weeks. Continuous PD treatment inhibited tumorigenesis, whereas its discontinuation resulted in high tumor counts (**Fig. 6g**). Collectively, these results indicate that the regulation of the ERK pathway in *Apc*$^{min/+}$ mice controls intestinal tumorigenesis and the subsequent manifestation of the Min phenotype, most likely by post-translational modifications of c-Myc protein.

DISCUSSION

Overt inflammation can promote neoplasia[29–32]. TLR activation of innate immune cells (for example, macrophages) in the intestinal mucosa triggers the production of various pro-inflammatory mediators[3,5]. This mechanism was proposed to enhance tumorigenesis in the *Apc*$^{min/+}$ mice[6]. However, our study indicates that in non-hematopoietic cells, such as IECs, MyD88 is required for intestinal tumor growth in the *Apc*$^{min/+}$ mouse. Furthermore, we found that TLR ligands, presumably from intestinal flora (**Fig. 4**) and not from the host (**Fig. 2**), mediate IEC tumor growth under steady-state conditions. In this setting, MyD88-mediated signaling induces ERK activation that stabilizes and thus increases the abundance of the Myc protein, the product of the oncogene *Myc* (*c-Myc*), in IECs[23]. This sequence of events enhances IEC proliferation and reduces IEC apoptosis and therefore promotes IEC tumor growth in *Apc*$^{min/+}$ mice.

The oncogene *Myc* is a Wnt target gene[33,34]. Although β-catenin–TCF signaling induces *Myc* transcriptionally, the gene's expression levels are heavily regulated by ubiquitin-mediated proteasomal degradation[35,36], which can be antagonized by p-ERK phosphorylation of c-Myc[23–25]. Our findings indicate that MyD88-dependent activation of ERK is necessary to stabilize c-Myc levels (**Fig. 4**); that the activation of ERK by the MyD88-independent ligand EGF[37] increases expression of c-Myc and restores the Min phenotype in *Apc*$^{min/+}$/*Myd88*$^{-/-}$ mice (**Fig. 5**); and that treatment with a specific ERK inhibitor suppresses tumor development in both *Apc*$^{min/+}$ and EGF-treated *Apc*$^{min/+}$/*Myd88*$^{-/-}$ mice (**Figs. 5** and **6**). Collectively, these data indicate that (i) loss of heterozygosity of *Apc* is insufficient to drive the Min phenotype in the *Apc*$^{min/+}$ mouse, (ii) synergy between c-Myc transcription and post-translational modifications is required for tumor growth in this model, (iii) activation of ERK is necessary for IEC tumorigenesis in the *Apc*$^{min/+}$ mouse and (iv) ERK functions as a major regulator of c-Myc expression in the intestinal epithelium (**Fig. 6h**).

Oncogene addiction is a mechanism that explains tumor suppression due to the inactivation of a single gene product. This phenomenon occurs when tumors require sustained activation of a single oncogene for their growth and survival, despite other oncogenic events[9]. Our data reveal that IEC tumor growth in the *Apc*$^{min/+}$ mice is due to p-ERK addiction. ERK addiction was also recently shown to drive the survival of certain intestinal epithelial cell lines *in vitro*[38], although by a different pathway. Activation of ERK in this setting is most likely induced by a TLR-MyD88–dependent pathway (for example, microflora) (**Fig. 3**) and by a TLR-MyD88–independent pathway (for example, growth factors) (**Fig. 5**). Consequently, the inhibition of ERK prevents tumorigenesis in *Apc*$^{min/+}$ mice, most likely through the generation of an unstable c-Myc protein (**Figs. 5** and **6**), leading to low c-Myc abundance in IECs (**Fig. 3**). Although regulation of the ERK–c-Myc pathway inhibits the Min phenotype under steady-state conditions, we cannot rule out other anti-apoptotic effects caused by p-ERK that may influence the Min phenotype[38]. The disparity in tumor numbers between *Apc*$^{min/+}$ and *Apc*$^{min/+}$/*Myd88*$^{-/-}$ mice (**Supplementary Fig. 1**), as well as the biochemical evidence presented above *in vitro* (**Fig. 4**) and *in vivo* (**Figs. 5** and **6**), strongly support the inductive role of microflora-derived MyD88 signaling on IEC tumorigenesis in *Apc*$^{min/+}$ mice. These observations suggest a new facet of oncogene-environment interactions, which might explain why a germline mutation in *Apc* results primarily in tumors originating in the intestinal epithelium (**Fig. 6h**) and not in other organs. Because p-ERK is important in the induction of the Min phenotype (**Figs. 5** and **6**), we propose that interventions aimed at inhibiting ERK activation in IECs (**Fig. 6**) may help suppress the induction of IEC neoplasia in humans with variant *APC* genes.

METHODS

Methods and any associated references are available in the online version of the paper at http://www.nature.com/naturemedicine/.

Note: Supplementary information is available on the Nature Medicine website.

ACKNOWLEDGMENTS

The authors thank P. Charos for animal breeding and S. Shenouda for tissue processing. This work was supported by US National Institutes of Health grants AI068685, CA133702, DK35108 and DK080506.

AUTHOR CONTRIBUTIONS

E.R. designed the study; S.H.L. and J.L. performed the signaling experiments; C.S., L.-L.H., S.H. and G.S.S. performed the *in vivo* studies; M.C. generated the bone marrow chimeras; J.B., J.L. and J.G.-N. performed immunohistochemistry and flow cytometry; S.H.L., M.C., N.V., J.L. and E.R. analyzed the data; and S.H.L., J.L. and E.R. wrote the manuscript.

COMPETING FINANCIAL INTERESTS

The authors declare that they have no competing financial interest.

Published online at http://www.nature.com/naturemedicine/.
Reprints and permissions information is available online at http://npg.nature.com/reprintsandpermissions/.

1. Michelsen, K.S. & Arditi, M. Toll-like receptors and innate immunity in gut homeostasis and pathology. *Curr. Opin. Hematol.* **14**, 48–54 (2007).
2. Sanderson, I.R. & Walker, W.A. TLRs in the Gut I. The role of TLRs/Nods in intestinal development and homeostasis. *Am. J. Physiol. Gastrointest. Liver Physiol.* **292**, G6–G10 (2007).
3. de Visser, K.E., Eichten, A. & Coussens, L.M. Paradoxical roles of the immune system during cancer development. *Nat. Rev. Cancer* **6**, 24–37 (2006).
4. Karin, M. Nuclear factor-κB in cancer development and progression. *Nature* **441**, 431–436 (2006).
5. Lin, W.W. & Karin, M. A cytokine-mediated link between innate immunity, inflammation, and cancer. *J. Clin. Invest.* **117**, 1175–1183 (2007).
6. Rakoff-Nahoum, S. & Medzhitov, R. Regulation of spontaneous intestinal tumorigenesis through the adaptor protein Myd88. *Science* **317**, 124–127 (2007).
7. Oshima, M. *et al.* Loss of Apc heterozygosity and abnormal tissue building in nascent intestinal polyps in mice carrying a truncated Apc gene. *Proc. Natl. Acad. Sci. USA* **92**, 4482–4486 (1995).
8. Moser, A.R., Pitot, H.C. & Dove, W.F. A dominant mutation that predisposes to multiple intestinal neoplasia in the mouse. *Science* **247**, 322–324 (1990).
9. Weinstein, I.B. Cancer. Addiction to oncogenes—the Achilles heal of cancer. *Science* **297**, 63–64 (2002).
10. Hurlin, P.J. & Huang, J. The MAX-interacting transcription factor network. *Semin. Cancer Biol.* **16**, 265–274 (2006).
11. Wilkins, J.A. & Sansom, O.J. C-Myc is a critical mediator of the phenotypes of Apc loss in the intestine. *Cancer Res.* **68**, 4963–4966 (2008).
12. Sansom, O.J. *et al.* Myc deletion rescues Apc deficiency in the small intestine. *Nature* **446**, 676–679 (2007).
13. Yekkala, K. & Baudino, T.A. Inhibition of intestinal polyposis with reduced angiogenesis in Apc$^{min/+}$ mice due to decreases in c-Myc expression. *Mol. Cancer Res.* **5**, 1296–1303 (2007).
14. Ignatenko, N.A. *et al.* Role of c-Myc in intestinal tumorigenesis of the Apcmin/+ mouse. *Cancer Biol. Ther.* **5**, 1658–1664 (2006).
15. Beutler, B. *et al.* Genetic analysis of host resistance: Toll-like receptor signaling and immunity at large. *Annu. Rev. Immunol.* **24**, 353–389 (2006).
16. Boulares, A.H. *et al.* Role of poly(ADP-ribose) polymerase (PARP) cleavage in apoptosis. Caspase 3-resistant PARP mutant increases rates of apoptosis in transfected cells. *J. Biol. Chem.* **274**, 22932–22940 (1999).
17. Kelsall, B.L. & Rescigno, M. Mucosal dendritic cells in immunity and inflammation. *Nat. Immunol.* **5**, 1091–1095 (2004).

18. Cario, E. *et al.* Commensal-associated molecular patterns induce selective toll-like receptor-trafficking from apical membrane to cytoplasmic compartments in polarized intestinal epithelium. *Am. J. Pathol.* **160**, 165–173 (2002).
19. Lee, J. *et al.* Maintenance of colonic homeostasis by distinctive apical TLR9 signalling in intestinal epithelial cells. *Nat. Cell Biol.* **8**, 1327–1336 (2006).
20. Cho, H.J. *et al.* IFN-alpha beta promote priming of antigen-specific $CD8^+$ and $CD4^+$ T lymphocytes by immunostimulatory DNA-based vaccines. *J. Immunol.* **168**, 4907–4913 (2002).
21. Apte, R.N. *et al.* The involvement of IL-1 in tumorigenesis, tumor invasiveness, metastasis and tumor-host interactions. *Cancer Metastasis Rev.* **25**, 387–408 (2006).
22. Pedersen, G., Andresen, L., Matthiessen, M.W., Rask-Madsen, J. & Brynskov, J. Expression of Toll-like receptor 9 and response to bacterial CpG oligodeoxynucleotides in human intestinal epithelium. *Clin. Exp. Immunol.* **141**, 298–306 (2005).
23. Sears, R. *et al.* Multiple Ras-dependent phosphorylation pathways regulate Myc protein stability. *Genes Dev.* **14**, 2501–2514 (2000).
24. Sears, R.C. The life cycle of C-myc: from synthesis to degradation. *Cell Cycle* **3**, 1133–1137 (2004).
25. Vervoorts, J., Luscher-Firzlaff, J. & Luscher, B. The ins and outs of MYC regulation by posttranslational mechanisms. *J. Biol. Chem.* **281**, 34725–34729 (2006).
26. Chang, W.C. *et al.* Sulindac sulfone is most effective in modulating beta-catenin-mediated transcription in cells with mutant APC. *Ann. NY Acad. Sci.* **1059**, 41–55 (2005).
27. Barrett, S.D. *et al.* The discovery of the benzhydroxamate MEK inhibitors CI-1040 and PD 0325901. *Bioorg. Med. Chem. Lett.* **18**, 6501–6504 (2008).
28. Seo, T.C., Spallholz, J.E., Yun, H.K. & Kim, S.W. Selenium-enriched garlic and cabbage as a dietary selenium source for broilers. *J. Med. Food* **11**, 687–692 (2008).
29. Coussens, L.M. & Werb, Z. Inflammation and cancer. *Nature* **420**, 860–867 (2002).
30. Shacter, E. & Weitzman, S.A. Chronic inflammation and cancer. *Oncology* **16**, 217–226, 229; discussion 230–232 (2002).
31. Fox, J.G. & Wang, T.C. Inflammation, atrophy, and gastric cancer. *J. Clin. Invest.* **117**, 60–69 (2007).
32. Pikarsky, E. *et al.* NF-κB functions as a tumour promoter in inflammation-associated cancer. *Nature* **431**, 461–466 (2004).
33. He, T.C. *et al.* Identification of c-MYC as a target of the APC pathway. *Science* **281**, 1509–1512 (1998).
34. Dang, C.V. *et al.* The c-Myc target gene network. *Semin. Cancer Biol.* **16**, 253–264 (2006).
35. Hann, S.R. Role of post-translational modifications in regulating c-Myc proteolysis, transcriptional activity and biological function. *Semin. Cancer Biol.* **16**, 288–302 (2006).
36. Gregory, M.A. & Hann, S.R. c-Myc proteolysis by the ubiquitin-proteasome pathway: stabilization of c-Myc in Burkitt's lymphoma cells. *Mol. Cell. Biol.* **20**, 2423–2435 (2000).
37. Dakour, J., Li, H., Chen, H. & Morrish, D.W. EGF promotes development of a differentiated trophoblast phenotype having c-myc and junB proto-oncogene activation. *Placenta* **20**, 119–126 (1999).
38. Wickenden, J.A. *et al.* Colorectal cancer cells with the BRAF(V600E) mutation are addicted to the ERK1/2 pathway for growth factor-independent survival and repression of BIM. *Oncogene* **27**, 7150–7161 (2008).
39. Sansom, O.J. *et al.* Loss of Apc in vivo immediately perturbs Wnt signaling, differentiation, and migration. *Genes Dev.* **18**, 1385–1390 (2004).
40. Dove, W.F. *et al.* Intestinal neoplasia in the ApcMin mouse: independence from the microbial and natural killer (beige locus) status. *Cancer Res.* **57**, 812–814 (1997).

ONLINE METHODS

Materials. The following antibodies were obtained from Cell Signaling Technology: anti–phospho-ERK1/2, anti-ERK1/2, anti–c-Myc, anti-PARP, anti–β-catenin, anti-PCNA and anti-MyD88. Anti-ubiquitin antibody was purchased from Santa Cruz Biotechnology and anti–phospho-c-Myc (Ser62) antibody for immunoblotting and anti–c-Myc antibody for immunohistochemistry from Abcam. InSolution MG-132 was purchased from Calbiochem, the MEK1/2 inhibitor (U0126) from Promega and the MEK1/2 inhibitor PD0325901 from Stemgent. Anakinra was purchased from Amgen, recombinant mEGF from PeproTech, Pam3Cys (P3C) from InvivoGen and Wnt3a from R&D Systems.

Mice. C57Bl/6J, *Apc*$^{min/+}$ and *Il1r1*$^{-/-}$ mice were purchased from The Jackson Laboratory. *Myd88*$^{-/-}$ mice were kindly provided by S. Akira (Osaka Univ., Osaka, Japan), and were backcrossed ten generations onto C57Bl/6, *Lps2* mice by B. Beutler (Scripps Research Institute, San Diego, California, USA) and *Casp1*$^{-/-}$ mice by R. Flavell (Yale Univ., New Haven, Connecticut, USA). All mouse strains were crossed to *Apc*$^{min/+}$ mice. All animal protocols received prior approval by the Institutional Review Board.

***In vivo* treatment with anakinra.** Eight- to ten-week-old mice *Apc*$^{min/+}$ mice were injected i.p. with 50 mg kg^{-1} of anakinra five times per week for 10 weeks and analyzed at 20 weeks of age.

***In vivo* treatment with EGF.** Eight- to ten-week-old mice were injected i.p. with EGF (2 μg per mouse) three times per week for 10 weeks and analyzed at 20 weeks of age.

***In vivo* treatment with an ERK inhibitor.** PD0325901 was dissolved initially in DMSO (50 mg ml^{-1}) as a stock solution. The stock solution was then diluted in water containing 0.05% (hydroxypropyl)methylcellulose and 0.02% Tween 80. The formulation containing PD0325901 in 250 μl at the 25 mg kg^{-1} dose was administered by gavage three times a week to EGF-treated *Apc*$^{min/+}$/*Myd88*$^{-/-}$ mice or five times a week to *Apc*$^{min/+}$ mice for the duration of each study. Control mice were treated with vehicle (gavage).

Bone marrow chimeras. Chimeras were generated by reconstituting irradiated (9 Gy of γ-radiation) 6- to 10-week-old *Apc*$^{min/+}$ and *Apc*$^{min/+}$/*Myd88*$^{-/-}$ mice with bone marrow cells (1.5×10^7, intravenously) from sex-matched WT or *Myd88*$^{-/-}$ donor mice. Chimerism was verified by quantitative PCR (qPCR) of peripheral blood cells. Polyp counts were performed when mice reached 20 weeks of age.

BrdU staining. Staining was performed using a BrdU *in situ* staining kit (BD Biosciences). Mice were injected i.p. with 2 mg of BrdU solution. Intestinal tissue samples were fixed with formalin and embedded in paraffin. Immunostaining for labeled BrdU was performed according to the manufacturer's instruction. Enumeration of BrdU positioning was performed as described[39].

TUNEL assay. The assay was performed on paraffinized intestinal tissues according to the manufacturer's instruction (BD Biosciences). Nuclei were stained with Hoechst 33258 (Invitrogen).

Isolation of intestinal epithelial cells, RT-PCR, immunoblotting and immunoprecipitation. These procedures were performed as previously described[19].

Cell culture. The human IEC lines RKO and Caco-2 were cultured in DMEM supplemented with 4.0 mM glutamine, 10% FCS, 50 U ml^{-1} penicillin and 50 μg ml^{-1} streptomycin.

siRNA-mediated knockdown. *Myd88* siRNA or *Myc* siRNA from Santa Cruz Biotechnology. Briefly, siRNA (40 μM) in 50 μl of Opti-MEM (Invitrogen) was mixed with 5 μl of Dharmafect 4 (Dharmacon) in 50 μl of Opti-MEM. After 30 min incubation at room temperature (22–25 °C), the transfection mixture was combined with 1×10^6 cells in culture medium. Non-targeting siRNA #2 (a luciferase-targeting siRNA) from Dharmacon was used as a control.

Histology and immunohistochemistry (IHC). DSI and colon were fixed in 10% formalin, paraffin embedded, and sectioned at 3–6 μm for H&E staining or immunostaining. The tissue sections were incubated overnight at 4 °C with rabbit anti–c-Myc antibody (1:50), rabbit anti–p-ERK antibody, or control antibody. After washing with PBS, sections were incubated in horseradish peroxidase–conjugated secondary antibody for 1 h, and the staining was visualized with the AEC peroxidase substrate kit (Vector Laboratories), with hematoxylin nuclear counterstaining.

Blood hemoglobin. Blood hemoglobin was measured on a MS9 Blood Analyzer (Melet Schloesing Laboratories) according to the manufacturer's instructions.

Statistical analysis. Statistical analyses were performed by Student's *t* test for paired samples or two-way analysis of variance for multiple comparisons and by log-rank analysis for survival curves. Data are presented as means ± s.d.